

Learning and Transferring Better with Depth Information in Visual Reinforcement Learning

Zichun Xu¹, Yuntao Li¹, Zhaomin Wang¹, Lei Zhuang¹, Guocai Yang², and Jingdong Zhao^{1,*}

Abstract—Depth information is robust to scene appearance variations and inherently carries 3D spatial details. In this paper, a visual backbone based on the vision transformer is proposed to fuse RGB and depth modalities for enhancing generalization. Different modalities are first processed by separate CNN stems, and the combined convolutional features are delivered to the scalable vision transformer to obtain visual representations. Moreover, a contrastive unsupervised learning scheme is designed with masked and unmasked tokens to accelerate the sample efficiency during the reinforcement learning process. For sim2real transfer, a flexible curriculum learning schedule is developed to deploy domain randomization over training processes.

Index Terms—Visual Reinforcement Learning, Representation Learning, Sim2Real

I. INTRODUCTION

Reinforcement learning (RL) has exhibited its superior ability in addressing contact-rich tasks without a tedious dynamics model. Recent works focus on integrating different modality information tailored to specific task scenarios, in which vision [1], proprioception [2], force/torque [3], and tactile [4] are prevalent alternatives. Considering real-world situations and the cost of acquiring information, vision is gradually emerging as an essential modality. In contrast to state-based data, high-dimensional vision streams need to be encoded as compact representations via visual backbone. For this reason, pixel-based RL exhibits low sample efficiency, i.e., more environment steps are required to achieve the same performance level. Thus, several works have been devoted to improving the sample efficiency of visual RL [5], [6].

Nevertheless, the substantial training cost of visual RL still discourages training on real robots. Researchers try to save the training cost via sim2real or fine-tuning in reality [7], [8]. For the exploitation of visual information, a visual backbone pretrained on in-the-wild datasets has been demonstrated to be effective in extracting generalized representations across different conditions, which also contributes to improving sim2real success rates [9], [10]. However, generalizability is a relatively ambiguous metric for evaluating the visual backbone. Some works suggest that a vision backbone capable of extracting object- or agent-centric representations performs better in diverse environments, benefiting from its weak sensitivity to irrelevant environment distractors [11], [12]. RGB images and domain randomization are employed to narrow the gap between simulation and reality in previous

works [13], [14], which is limited to boost the transfer performance. Thus, other modalities are pursued for additional gains.

Compared to RGB images, depth information can better mitigate perceptual disparities and provide distance information to empower spatial awareness. Depth images enable more efficient online training than other forms of depth representations, e.g., point clouds, with less training burden. A common utilization of depth images is early fusion, in which depth is an extra channel of RGB images. Empirical evidence from computer vision demonstrates that the fusion strategy and framework for RGB-D play a pivotal role in semantic segmentation, revealing that channel-wise concatenation cannot fully unleash the power of depth information. Inspired by the above, this paper introduces a deeper fusion paradigm with the self-attention mechanism of the vision transformer (ViT) [15]. We also compare and analyze multiple approaches for fusing depth information. Extensive simulation experiments demonstrate that the proposed vision backbone can better utilize the depth information and thus improve the sample efficiency and generalization. In summary, our contributions are threefold:

- 1) We propose a lightweight backbone based on ViT to fuse RGB-D information. The trained vision backbone demonstrates the capability to extract object- and agent-centric representations while effectively exploiting the complementary advantages of each modality.
- 2) The contrastive learning scheme is configured with masked and unmasked tokens encoded by ViT to enhance the sample efficiency.
- 3) Visual backbone and policy network trained through curriculum-based domain randomization can be transferred to the real world in a zero-shot manner.

II. RELATED WORK

A. Visual RL

Visual RL is an intersection field spanning RL and computer vision. A prevalent framework is to integrate the training of the visual backbone with the policy network, which facilitates the extraction of in-domain features [16], [17]. For this training paradigm, limited visual diversity and unlabeled data highlight the importance of improving sample efficiency. Data augmentations [18], such as random shift and color jitter, can significantly enhance the sample efficiency and adaptability of the agent to unseen environments. Extra recipes are essential for stabilizing critic updates during training. Denis et al. proposed the renowned DrQ [19] and

¹State Key Laboratory of Robotics and Systems, Harbin Institute of Technology, Harbin 150001, Heilongjiang Province, China.

*Corresponding author: zhaojingdong@hit.edu.cn

its successor DrQv2 [20], which derive the critic target from weak augmented visual observations. While SVEA [21] allows weak and strong augmented observations to share the same critic target. In addition to meticulous recipes, visual backbone is also relevant to sample efficiency and visual attention regions. A CNN-based visual backbone is more preferred with its lightweight architecture compared to ViT. Some well-established vision architectures, such as ResNet18 [22] and ViT-B [15], are overweight for online RL despite being highly acclaimed in computer vision. Online RL requires frequent data interactions to continuously update the policy, and some large-scale model architectures, even pre-trained versions, consume much wall-clock time [23], [24], [25]. Scalable ViT and the first two layers of pre-trained ResNet18 have been validated as visual backbones for training off-policy algorithms [21], [10]. Therefore, for our work, a scaled ViT with two stems is constructed as the visual backbone to fuse RGB and depth information for online training.

B. Generalization in visuomotor control

RGB has become an indispensable option when training with visual modality [1], [26]. Like human binocular perception, RGB images enable faster comprehension of complex scenes through scene changes. The sim2real discrepancy persists despite photorealistic rendering and necessary domain randomization in some simulators. A robust visual backbone with strong generalization has a crucial impact on the sim2real transfer. Specifically, an ideal visual backbone focuses on task-relevant regions. Manipulation centricity [27] is proposed as an indicator to quantify the performance of trained visual backbones for downstream manipulation tasks. Pre-training on robot-related datasets [28] can better reduce the domain gap compared to those on daily-life datasets. Similarly, related works attempt to obtain disentangled or agent-related representations that perform robustly against distracting backgrounds [11], [12]. However, some sim2real works primarily treat RGB as the main modality while rarely utilizing depth information [29], [30]. The embedded distance information and the insensitivity to appearance variations are valuable properties of depth information for enhancing visual generalization. Injection of random noise during simulation followed by a denoising process is sufficient without elaborate domain randomization for depth information [31]. In this paper, we do not simply adopt the early fusion via channel concatenation. Instead, the self-attention mechanism of ViT is used to deeply exploit the depth modality.

III. PRELIMINARIES

A. Visual Reinforcement Learning

The visual RL process can be formulated as a partially observable Markov decision process (POMDP), defined as a tuple $\langle \mathcal{O}, \mathcal{A}, \mathcal{P}, \mathcal{R}, \rho, \gamma \rangle$ with visual observation space \mathcal{O} , action space \mathcal{A} , transition function $\mathbf{o}_{t+1} = \mathcal{P}(\cdot | \mathbf{o}_t, \mathbf{a}_t)$, reward function $r_t = \mathcal{R}(\mathbf{o}_t, \mathbf{a}_t)$, distribution of the initial state $\mathbf{o}_0 \sim \rho$, and discount factor $\gamma \in [0, 1)$. A stack

of recent frames are adopted as the current observation $\mathbf{o}_t = (\mathbf{x}_{t-i}, \dots, \mathbf{x}_t)$ to learn the temporal information. Our goal is training policies that maximize the cumulative reward $\mathbb{E}_\pi [\sum_{t=0}^{\infty} \gamma^t r_t]$ and finish the corresponding manipulation task.

B. Vision Transformer

ViT is an outstanding application to extend the self-attention in natural language processing to the field of computer vision. An image $\mathbf{o}_t \in \mathbb{R}^{H \times W \times C}$ is split into $N = HW/P^2$ non-overlapping patches $p_n \in \mathbb{R}^{N \times (P^2 \cdot C)}$ and expanded into a 1-dimensional sequence. The CLS token is integrated in the patch sequence, and the position embeddings $E_{pos} \in \mathbb{R}^{(N+1) \times D}$ are added for the preservation of the positional information

$$\mathbf{z}_e^0 = [T_{CLS}; p_1; \dots; p_N] + E_{pos}. \quad (1)$$

The transformer encoder consists of L identical layers, each of which includes the multihead self-attention (MSA) and feed-forward (FFN) blocks. The input vector $\mathbf{z}_e^{i-1} \in \mathbb{R}^{N \times D}$, $i = 0 \dots L$ to MSA is first linearly mapped into query, key, and value, i.e., $Q, K, V \in \mathbb{R}^{h \times N \times D_h}$. The attention score is then derived with

$$O_{ij} = \text{softmax} \left(\frac{Q_{ij} K_{ij}^T}{\sqrt{D_h}} \right) \cdot V_{ij} \quad j = 1 \dots h \quad (2)$$

and added with \mathbf{z}_e^{i-1} through the residual connection. The entire encoding process with FFN can be summarized as

$$\begin{aligned} \mathbf{z}_e^i &= \text{MSA}(\text{LayerNorm}(\mathbf{z}_e^{i-1})) + \mathbf{z}_e^{i-1} \\ \mathbf{z}_e^i &= \text{FFN}(\text{LayerNorm}(\mathbf{z}_e^i)) + \mathbf{z}_e^i \\ \mathbf{z}_e^L &= \text{LayerNorm}(\mathbf{z}_e^L) \end{aligned} \quad (3)$$

The CLS token of \mathbf{z}_e^L can be treated as the visual representation \mathbf{z}_t for downstream RL [21]. Masked autoencoder (MAE) [32] is a self-supervised learning scheme that builds upon ViT. Random patches are masked, and the remaining portion is utilized to construct the latent, which is then employed by the decoder to reconstruct the original image.

IV. METHOD

This section presents a visual backbone based on ViT to fuse RGB and depth images for visual RL. The proposed visual backbone can be integrated into the popular off-policy RL framework to extract the representation that embeds multimodal visual information. To further improve the generalizability and the perception of task-related regions, a contrastive self-supervised learning scheme is designed in light of the random masking of MAE. Details will be given in the following sections.

A. Multimodal Visual Encoder

ViT is commonly used to encode RGB images. For the depth stream, we refer to [33] to build another stem to split the stack of depth images, which is shown in Fig. 1. Meanwhile, prior studies have indicated that early convolutions before feeding to the ViT help to capture fine-grained details.

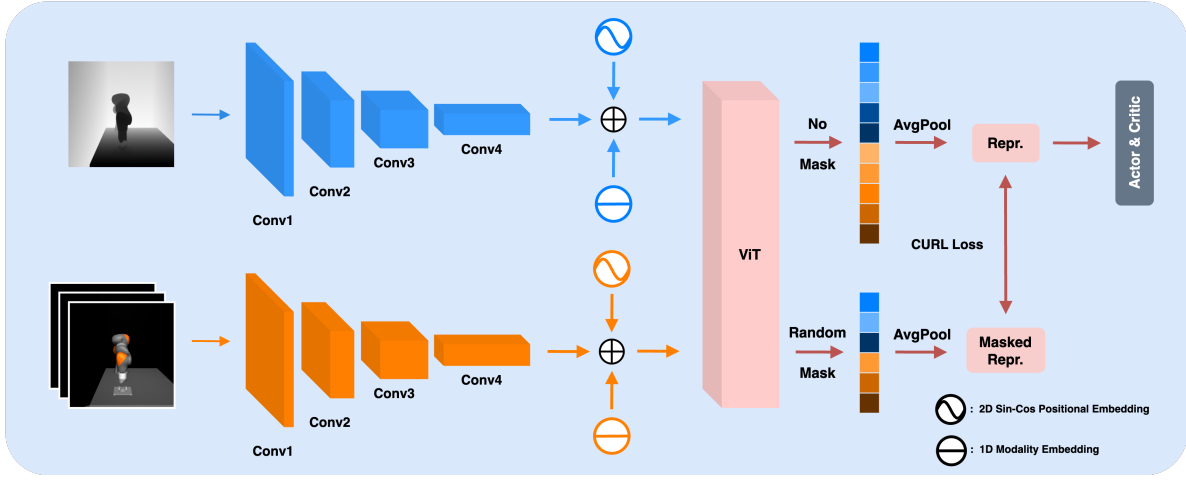


Fig. 1. Overview of our approach. We build a visual backbone with two CNN stems to process RGB and depth images, respectively. The convoluted features are concatenated and then passed to ViT to obtain encoded tokens. Average pooling is applied to the unmasked tokens to derive compact visual embeddings for the policy head. Concurrently, contrastive training is performed using masked and unmasked tokens. Trained visual and policy networks are frozen and transferred to reality without fine-tuning.

Thus, RGB and depth image are processed separately via the corresponding convolution stems:

$$\mathbf{h}_t^{rgb} = g_{conv}^{rgb}(\mathbf{o}_t^{rgb}) \quad \mathbf{h}_t^d = g_{conv}^d(\mathbf{o}_t^d) \quad (4)$$

Individual 2D sin-cos position and 1D modality embeddings are added to the convoluted features, respectively. Embedding vectors of different modalities are concatenated and passed to ViT (g_v). The visual representation can be obtained by the average-pooling operation on the encoded tokens without an additional MLP head:

$$\mathbf{z}_t = \text{AvgPool}\left(g_v\left(\left[\mathbf{h}_t^{rgb}; \mathbf{h}_t^d\right]\right)\right) \quad (5)$$

The encoded tokens can also be randomly masked and transmitted to an asymmetric decoder to reconstruct the unmasked images of different modalities, which is the implementation of MAE. A research [33] similar to ours reconstructs RGB and tactile observations, in which the effect of the decoder on the performance of extracted visual representation is not discussed. On this point, subsequent simulation results will explore the effect of the asymmetric decoder on sample efficiency and generalizability for RL.

B. Contrastive Learning

Contrastive unsupervised learning [34] (CURL) aims to maximize the mutual information between the anchor and target. For applications in visual RL, the query and key of the latent representation can be derived by the visual encoder and span different viewpoints [35] or temporal dimensions [36]. Moreover, CURL contributes to improving the sample efficiency. Inspired by CURL and MAE, masked and unmasked image patches naturally form the anchor and target parts of CURL. Unlike MAE, random masking is performed on the convolutional features instead of normalized images and performed uniformly over two visual modalities. Random shuffle is not executed after random masking since there is no asymmetric decoder. Note that random masking is

only available to the CURL phase. The visual representation employed by the actor and critic is unmasked. The loss function of CURL can be represented as

$$\mathcal{L}_{curl} = -\alpha \log \frac{\exp(q^T \cdot k^+ / \tau)}{\exp(q^T \cdot k^+ / \tau) + \sum_- \exp(q^T \cdot k^- / \tau)} \quad (6)$$

where τ is the temperature coefficient. Query $q = \mathbf{h}_t$ and key $k^+ \sim p^{mask}(\mathbf{h}_t^{mask} | [\mathbf{h}_t^{rgb}; \mathbf{h}_t^d], m)$. α is the contrastive loss weight, and m is the masking ratio. In contrast to the original CURL [34], the query-key pair is generated not by the target network for the visual encoder but instead by the recent weights.

C. Reinforcement Learning Backbone

The proposed visual encoder and contrastive learning process are integrated into the DrQ-v2 [20] framework, which is an extension of DDPG [37] for visual RL. N -step returns and the clipped-double Q trick are adopted to reduce the temporal difference error and the overestimation bias of target Q-value. Weak augmentation, i.e., random shift, is employed in DrQ-v2 to acquire the augmented data, which is limited for improving visual generalization. This paper aims to transfer the trained visual backbone and policy network to reality in a zero-shot manner. Thus, strong-augmented observations used in this paper are obtained by randomly overlaying with out-of-domain images. Besides, the original data augmentation recipe in DrQ-v2 is replaced with SVEA [21] to further improve visual generalization and stabilize the training process. Given the batch data $\mathcal{B} = (\mathbf{o}_t, \mathbf{a}_t, r_{t:t+n-1}, \mathbf{o}_{t+n})$ from the replay buffer \mathcal{D} , the actor is updated with the following loss:

$$\mathcal{L}_\pi = -\mathbb{E}_{\mathcal{B} \sim \mathcal{D}} \left[\min_{k=1,2} Q_{\theta_k}(f_\xi(\mathbf{o}_t), \tilde{\mathbf{a}}_t) \right], \quad (7)$$

where f_ξ indicates the vision encoder. $\tilde{\mathbf{a}}_t = \pi_\phi(f_\xi(\mathbf{o}_t)) + \epsilon$ is inferred by the policy network only with the weak aug-

Algorithm 1 Training details

Require: Policy π_θ , critics Q_{θ_k} , visual encoder f_ξ , learning rate η , replay buffer \mathcal{D} , training steps T , evaluation period E , mask ratio m , contrastive loss weight α , decay coefficient λ , domain randomization flag p_f , and CURL frequency F .

```
1:  $s_0 \leftarrow \rho$ 
2: for timesteps  $t = 1 \dots T$  do
3:    $\tilde{\mathbf{a}}_t \leftarrow \pi_\phi(\cdot | \mathbf{o}_t)$ 
4:    $\mathbf{o}_{t+1} \leftarrow \mathcal{P}(\cdot | \mathbf{o}_t, \tilde{\mathbf{a}}_t)$ 
5:    $\mathcal{D} \leftarrow \mathcal{D} \cup (\mathbf{o}_t, \tilde{\mathbf{a}}_t, r_t, \mathbf{o}_{t+1})$ 
6:    $\mathcal{B} \leftarrow \mathcal{D}$   $\triangleright$  Sample batch transitions
7:   UPDATECRITIC( $\mathcal{B}$ ) with Eq. 8
8:   UPDATEACTOR( $\mathcal{B}$ ) with Eq. 7
9:   if  $t \% F == 0$  then
10:    CURL with Eq. 6  $\triangleright$  Update Visual Encoder
11:   end if
12:   if  $t \% E == 0$  then
13:      $p_{eval} \leftarrow$  Evaluations
14:     if  $p_{eval} \geq p_f$  then
15:       Domain randomization enabled
16:     end if
17:   end if
18: end for
```

mented stream. ϵ is the exploration noise. $\mathbf{o}_t^{\text{aug}}$ denotes the observation after the strong augmentation. The critic loss is defined with both weak and strong augmented streams:

$$\mathcal{L}_Q = \mathbb{E}_{\mathcal{B} \sim \mathcal{D}} \left[\beta_1 \left\| Q_{\theta_k}(f_\xi(\mathbf{o}_t), \mathbf{a}_t) - y_t^{\text{tgt}} \right\|_2^2 + \beta_2 \left\| Q_{\theta_k}(f_\xi(\mathbf{o}_t^{\text{aug}}), \mathbf{a}_t) - y_t^{\text{tgt}} \right\|_2^2 \right] \quad \forall k \in \{1, 2\}, \quad (8)$$

where

$$y_t^{\text{tgt}} = \sum_{i=0}^{n-1} \gamma^i r_{t+i} + \gamma^n \left(\min_{k=1,2} Q_{\theta_k}(f_\xi(\mathbf{o}_{t+n}), \tilde{\mathbf{a}}_{t+n}) \right) \quad (9)$$

is the critic target obtained only with unaugmented observation. β_1 and β_2 are utilized to balance the two data streams.

D. Curriculum-based Domain Randomization

Domain randomization is incorporated into the training process to reduce the sim2real gap, encompassing variations in scene appearance, lighting conditions, dynamics parameters, and camera viewpoints. Large randomized magnitude will trigger divergence in the RL process. Thus, we implement a curriculum-based domain randomization approach inspired by [31] to progressively broaden the random range. When domain randomization initiates, the random ranges of all parameters expand exponentially with increasing episodes

$$R_{curr} = R_{def} * \lambda + R_{range} * (1 - \lambda^{T_e}), \quad (10)$$

where R_{curr} and R_{def} are randomized and default domain parameters, respectively. R_{range} represents the predefined random range. λ is the decay coefficient over running

episodes T_e . However, domain randomization is invoked when a fixed number of training frames is achieved in [31], which is an empirical determinant for different tasks. A more flexible determinant is adopted in this paper, i.e., the evaluation success rate. Such a metric prevents training divergence and unnecessary computational overhead caused by either premature or delayed initiation of domain randomization. Algorithm 1 provides a detailed explanation about the training process.

REFERENCES

- [1] W. Chen, C. Zeng, H. Liang, F. Sun, and J. Zhang, "Multimodality Driven Impedance-Based Sim2Real Transfer Learning for Robotic Multiple Peg-in-Hole Assembly," *IEEE Transactions on Cybernetics*, pp. 1–14, 2024.
- [2] S. Noh and H. Myung, "Toward Effective Deep Reinforcement Learning for 3d Robotic Manipulation: Multimodal End-to-End Reinforcement Learning from Visual and Proprioceptive Feedback," in *Deep Reinforcement Learning Workshop NeurIPS 2022*, 2022.
- [3] P. Jin, B. Huang, W. W. Lee, T. Li, and W. Yang, "Visual-Force-Tactile Fusion for Gentle Intricate Insertion Tasks," *IEEE Robotics and Automation Letters*, pp. 1–8, 2024.
- [4] J. Hansen, F. Hogan, D. Rivkin, D. Meger, M. Jenkin, and G. Dudek, "Visuotactile-RL: Learning Multimodal Manipulation Policies with Deep Reinforcement Learning," in *2022 International Conference on Robotics and Automation (ICRA)*. IEEE, 2022, pp. 8298–8304.
- [5] G. Xu, R. Zheng, Y. Liang, X. Wang, Z. Yuan, T. Ji, Y. Luo, X. Liu, J. Yuan, P. Hua, S. Li, Y. Ze, H. D. III, F. Huang, and H. Xu, "Drm: Mastering Visual Reinforcement Learning through Dormant Ratio Minimization," in *International Conference on Learning Representations (ICLR)*, 2024.
- [6] G. Ma, L. Zhang, H. Wang, L. Li, Z. Wang, Z. Wang, L. Shen, X. Wang, and D. Tao, "Learning Better with Less: Effective Augmentation for Sample-Efficient Visual Reinforcement Learning," in *Conference on Neural Information Processing Systems (NeurIPS)*, 2023.
- [7] R. Julian, B. Swanson, G. S. Sukhatme, S. Levine, C. Finn, and K. Hausman, "Never stop learning: The effectiveness of fine-tuning in robotic reinforcement learning," *arXiv preprint arXiv:2004.10190*, 2020.
- [8] Y. Ze, N. Hansen, Y. Chen, M. Jain, and X. Wang, "Visual Reinforcement Learning With Self-Supervised 3d Representations," *IEEE Robotics and Automation Letters*, vol. 8, no. 5, pp. 2890–2897, 2023.
- [9] I. Radosavovic, T. Xiao, S. James, P. Abbeel, J. Malik, and T. Darrell, "Real-World Robot Learning with Masked Visual Pre-training," in *Conference on Robot Learning (CoRL)*. arXiv, 2022, pp. 416–426.
- [10] Z. Yuan, Z. Xue, B. Yuan, X. Wang, Y. Wu, Y. Gao, and H. Xu, "Pre-Trained Image Encoder for Generalizable Visual Reinforcement Learning," in *Conference on Neural Information Processing Systems (NeurIPS)*, 2022.
- [11] K. Gmelin, S. Bahl, R. Mendonca, and D. Pathak, "Efficient RL via Disentangled Environment and Agent Representations," in *International Conference on Machine Learning (ICML)*, 2023, pp. 11 525–11 545.
- [12] A. Pore, R. Muradore, and D. Dall'Alba, "DEAR: Disentangled Environment and Agent Representations for Reinforcement Learning without Reconstruction," in *2024 IEEE/RSJ International Conference on Intelligent Robots and Systems (IROS)*. IEEE, 2024, pp. 650–655.
- [13] X. B. Peng, M. Andrychowicz, W. Zaremba, and P. Abbeel, "Sim-to-Real Transfer of Robotic Control with Dynamics Randomization," in *2018 IEEE International Conference on Robotics and Automation (ICRA)*. IEEE, 2018, pp. 3803–3810.
- [14] J. Josifovski, M. Malmir, N. Klarmann, B. L. Žagar, N. Navarro-Guerrero, and A. Knoll, "Analysis of Randomization Effects on Sim2Real Transfer in Reinforcement Learning for Robotic Manipulation Tasks," in *2022 IEEE/RSJ International Conference on Intelligent Robots and Systems (IROS)*. IEEE, 2022, pp. 10 193–10 200.
- [15] A. Dosovitskiy, L. Beyer, A. Kolesnikov, D. Weissenborn, X. Zhai, T. Unterthiner, M. Dehghani, M. Minderer, G. Heigold, S. Gelly, J. Uszkoreit, and N. Houlsby, "An Image is Worth 16x16 Words: Transformers for Image Recognition at Scale," in *International Conference on Learning Representations (ICLR)*, 2021.

- [16] D. Bertoin, A. Zouitine, M. Zouitine, and E. Rachelson, "Look where you look! Saliency-guided Q-networks for generalization in visual Reinforcement Learning." in *Conference on Neural Information Processing Systems (NeurIPS)*, 2022.
- [17] Z. Yuan, S. Yang, P. Hua, C. Chang, K. Hu, and H. Xu, "RL-ViGen: A Reinforcement Learning Benchmark for Visual Generalization." in *Conference on Neural Information Processing Systems (NeurIPS)*, 2023.
- [18] M. Laskin, K. Lee, A. Stooke, L. Pinto, P. Abbeel, and A. Srinivas, "Reinforcement Learning with Augmented Data." in *Conference on Neural Information Processing Systems (NeurIPS)*, 2020.
- [19] D. Yarats, I. Kostrikov, and R. Fergus, "Image Augmentation Is All You Need: Regularizing Deep Reinforcement Learning from Pixels." in *International Conference on Learning Representations (ICLR)*, 2021.
- [20] D. Yarats, R. Fergus, A. Lazaric, and L. Pinto, "Mastering Visual Continuous Control: Improved Data-Augmented Reinforcement Learning." in *International Conference on Learning Representations (ICLR)*, 2022.
- [21] N. Hansen, H. Su, and X. Wang, "Stabilizing Deep Q-Learning with ConvNets and Vision Transformers under Data Augmentation." in *Conference on Neural Information Processing Systems (NeurIPS)*, 2021, pp. 3680–3693.
- [22] K. He, X. Zhang, S. Ren, and J. Sun, "Deep Residual Learning for Image Recognition." in *Computer Vision and Pattern Recognition (CVPR)*, 2016, pp. 770–778.
- [23] T. Xiao, I. Radosavovic, T. Darrell, and J. Malik, "Masked Visual Pre-training for Motor Control," *arXiv.org*, vol. abs/2203.06173, 2022.
- [24] S. Parisi, A. Rajeswaran, S. Purushwalkam, and A. Gupta, "The Unsurprising Effectiveness of Pre-Trained Vision Models for Control." in *International Conference on Machine Learning (ICML)*, 2022, pp. 17 359–17 371.
- [25] S. Nair, A. Rajeswaran, V. Kumar, C. Finn, and A. Gupta, "R3M: A Universal Visual Representation for Robot Manipulation." in *Conference on Robot Learning (CoRL)*, 2022, pp. 892–909.
- [26] R. Jangir, N. Hansen, S. Ghosal, M. Jain, and X. Wang, "Look Closer: Bridging Egocentric and Third-Person Views With Transformers for Robotic Manipulation," *IEEE Robotics and Automation Letters*, vol. 7, no. 2, pp. 3046–3053, 2022.
- [27] G. Jiang, Y. Sun, T. Huang, H. Li, Y. Liang, and H. Xu, "Robots pre-train robots: Manipulation-centric robotic representation from large-scale robot datasets," *arXiv preprint arXiv:2410.22325*, 2024.
- [28] A. Khazatsky, K. Pertsch, S. Nair, A. Balakrishna, S. Dasari, S. Karamcheti, S. Nasiriany, M. K. Srirama, L. Y. Chen, K. Ellis *et al.*, "Droid: A large-scale in-the-wild robot manipulation dataset," *arXiv preprint arXiv:2403.12945*, 2024.
- [29] C. Yuan, Y. Shi, Q. Feng, C. Chang, M. Liu, Z. Chen, A. C. Knoll, and J. Zhang, "Sim-to-Real Transfer of Robotic Assembly with Visual Inputs Using CycleGAN and Force Control," in *2022 IEEE International Conference on Robotics and Biomimetics (ROBIO)*. IEEE, 2022, pp. 1426–1432.
- [30] J. Tobin, R. Fong, A. Ray, J. Schneider, W. Zaremba, and P. Abbeel, "Domain randomization for transferring deep neural networks from simulation to the real world." in *IEEE/RJS International Conference on Intelligent Robots and Systems (IROS)*, 2017, pp. 23–30.
- [31] Z. Yuan, T. Wei, S. Cheng, G. Zhang, Y. Chen, and H. Xu, "Learning to Manipulate Anywhere: A Visual Generalizable Framework For Reinforcement Learning," in *Conference on Robot Learning (CoRL)*, 2024.
- [32] K. He, X. Chen, S. Xie, Y. Li, P. Dollar, and R. Girshick, "Masked Autoencoders Are Scalable Vision Learners," in *2022 IEEE/CVF Conference on Computer Vision and Pattern Recognition (CVPR)*. IEEE, 2022, pp. 15 979–15 988.
- [33] C. Sferrazza, Y. Seo, H. Liu, Y. Lee, and P. Abbeel, "The Power of the Senses: Generalizable Manipulation from Vision and Touch through Masked Multimodal Learning," in *2024 IEEE/RSJ International Conference on Intelligent Robots and Systems (IROS)*. IEEE, 2024, pp. 9698–9705.
- [34] M. Laskin, A. Srinivas, and P. Abbeel, "CURL: Contrastive Unsupervised Representations for Reinforcement Learning," in *International Conference on Machine Learning (ICML)*, 2020, pp. 5639–5650.
- [35] M. Dunion and S. V. Albrecht, "Multi-view Disentanglement for Reinforcement Learning with Multiple Cameras." in *Reinforcement Learning Conference (RLC)*, vol. 2, 2024, pp. 498–515.
- [36] R. Zheng, X. Wang, Y. Sun, S. Ma, J. Zhao, H. Xu, H. D. III, and F. Huang, "Taco: Temporal Latent Action-Driven Contrastive Loss for Visual Reinforcement Learning." in *Conference on Neural Information Processing Systems (NeurIPS)*, 2023.
- [37] T. P. Lillicrap, J. J. Hunt, A. Pritzel, N. Heess, T. Erez, Y. Tassa, D. Silver, and D. Wierstra, "Continuous control with deep reinforcement learning," in *International Conference on Learning Representations (ICLR)*, 2016.